Enhancing Eu^{3+} magnetic dipole emission by resonant plasmonic nanostructures

Rabia Hussain,[1] Sergey S. Kruk,[2] Carl E. Bonner,[1] Mikhail A. Noginov,[1] Isabelle Staude,[2] Yuri S. Kivshar,[2] Natalia Noginova,[1,3] and Dragomir N. Neshev[2,*]

[1]*Center for Materials Research, Norfolk State University, Norfolk, Virginia 23504, USA*

[2]*Nonlinear Physics Centre, Research School of Physics and Engineering, Australian National University, Canberra ACT 2601, Australia*

[3]*e-mail: nnoginova@nsu.edu*

**Corresponding author: Dragomir.Neshev@anu.edu.au*

Received December 17, 2014; revised February 26, 2015; accepted March 9, 2015; posted March 13, 2015 (Doc. ID 230842); published April 3, 2015

We demonstrate the enhancement of magnetic dipole spontaneous emission from Eu^{3+} ions by an engineered plasmonic nanostructure that controls the electromagnetic environment of the emitter. Using an optical microscope setup, an enhancement in the intensity of the Eu^{3+} magnetic dipole emission was observed for emitters located in close vicinity to a gold nanohole array designed to support plasmonic resonances overlapping with the emission spectrum of the ions. © 2015 Optical Society of America

OCIS codes: (300.2140) Emission; (310.6628) Subwavelength structures, nanostructures; (240.6680) Surface plasmons.

http://dx.doi.org/10.1364/OL.40.001659

The pioneering work of Purcell [1] has played a pivotal role in our understanding of the nature of spontaneous emission processes. It has shown that such processes are not only an intrinsic property of the emitter, but can also be strongly modified by resonant coupling to the electromagnetic environment. This has opened entirely new possibilities for the enhancement of emission from even weak sources. Nevertheless, while Purcell developed his work for the enhancement of the emission from a microwave magnetic dipole, the implementation of this concept in optics was mostly carried out using electric dipole emitters. These studies have created a huge arsenal of techniques for the control of the electromagnetic environment and, more specifically, the enhancement of the electric field near an emitter. However, the control of emission from optical magnetic dipoles remains largely unexplored.

Magnetic dipole transitions at optical frequencies are usually weak; however, the possibility to enhance the emission rates of such weak emitters has promised to open many applications, including display technologies, fluorescent bioprobes, and quantum light sources. Such possibilities have recently triggered renewed attention for the control of magnetic dipole emitters by photonic nanostructures [2–8]. However, most works to date have only focused on the use of simple nonresonant structures such as metal–dielectric stacks [2–6,9–17] and there are no experiments on the manipulation of magnetic dipole emission by engineered resonant nanostructures. The latter therefore represents an important milestone in the development of bright magnetic emitters. Here we present, for the first time to our knowledge, the enhancement of magnetic dipole emission by a resonant nanostructure with magnetic response. In particular, we use a thin layer of Eu^{3+} ions, which have closely adjacent magnetic and electric dipole emission lines, and place it over an array of nanoholes exhibiting plasmonic resonances in the Eu^{3+} emission range. We show an enhancement of the magnetic dipole with respect to the electric dipole emission due to the presence of the nanohole array.

The control of the magnetic environment at the nanoscale has experienced great progress in the past decade with the development of metamaterials possessing unique optical properties and desired electromagnetic responses [18]. In particular, with the recent development of magnetically resonant metallic [19] and high-index dielectric nanoparticles [20] at optical frequencies, the engineering of the magnetic environment promises important future developments. In fact, one of the simplest nanostructures for the control of the magnetic field is represented by a nanohole in a metal film. Such nanoholes have been proven to act as efficient probes of the magnetic field [21] and have been used for near-field magnetic field detection [22–25]. Therefore, nanoholes represent an attractive option for achieving a resonantly enhanced magnetic response.

In our experiments, we employ rare-earth metal ions, such as Eu^{3+} ions, having both electric and magnetic dipole transitions in their spontaneous emission spectra [2,4,12]. The spectroscopic properties of Eu^{3+} luminescence, here in $Eu(TTA)^3(L18)$ [an alkylated europium complex, tris(α-thenoyltrifluoroacetone)(1-octadecyl-2(-2-pyridyl) benzimidazole) europium(III)], are summarized in Fig. 1. Figure 1(a) depicts the energy-level diagram for the absorption and emission transitions between the $^5D_0$ and ^7F_n energy states of Eu^{3+}. Figures 1(b) and 1(c) show, respectively, the excitation and emission spectra of the $Eu(TTA)^3(L18)$ complex. The strongest excitation band occurs in the ultraviolet range with maximum absorption at around 330 nm. Importantly, the Eu^{3+} emission line at $\lambda \approx 590$ nm is associated primarily with a magnetic dipole transition $^5D_0 \rightarrow {}^7F_1$, whereas the strongest line in the emission spectrum at $\lambda \approx 611$ nm corresponds to an electric dipole transition $^5D_0 \rightarrow {}^7F_2$ [26]. The effects of the local optical environment on the electric and magnetic dipole emission have been studied theoretically and experimentally in the flat geometry [2–4,10–13]. Variation of the relaxation rate and the interplay of the relative intensities of the electric and

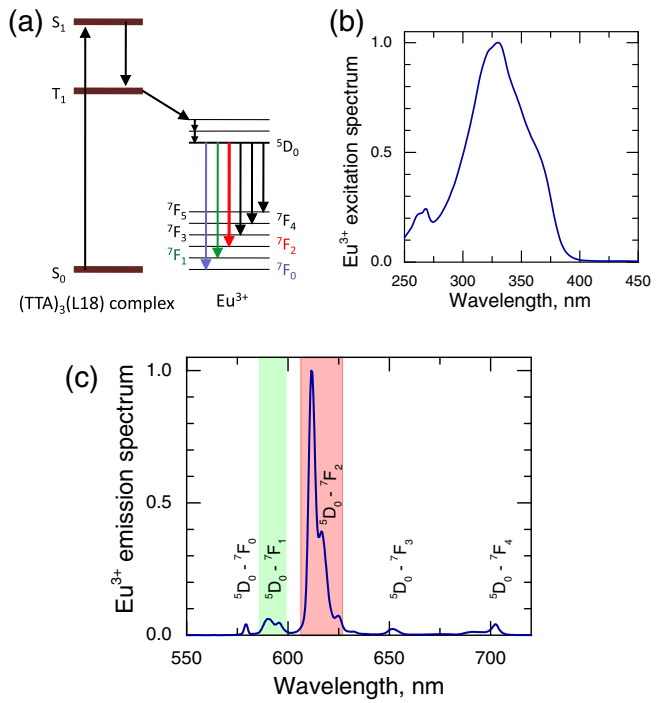

Fig. 1. Spectroscopic properties of Eu(TTA)^3(L18). (a) Energy-level diagram showing absorption and spontaneous emission transitions between the $^5D_0$ and ^7F_n energy states of Eu^{3+}; (b) excitation spectrum of Eu(TTA)^3(L18); and (c) emission spectrum recorded at 330 nm excitation.

magnetic dipole transitions have been observed as a function of the distance between the Eu^{3+} emitters and a plane mirror [3,13]. A reduction of the electric dipole emission and an enhancement of the magnetic dipole emission for emitters placed in the vicinity of an ideal electric mirror (perfect conductor) were predicted due to the boundary conditions for the electric and magnetic components of the optical fields [2,10]. However, the emission of Eu^{3+} in the vicinity of nanostructured resonant surfaces, especially those exhibiting artificial magnetism, has never been experimentally studied before.

To show how such metasurfaces can influence the emission from electric and magnetic dipoles, we design and fabricate a plasmonic nanohole array that supports a resonance in the spectral range of the Eu^{3+} magnetic dipole transition. A sketch of our experimental geometry is shown in Fig. 2(a). The samples (40 μm × 40 μm) are fabricated by focused-ion beam milling of a 150 nm thick gold film deposited on a glass substrate. Nanoholes with sizes 200 nm × 280 nm were arranged into a square array with 400 nm lattice constant. A scanning electron micrograph (SEM) image of the fabricated sample is shown in Fig. 2(b). The fabricated nanohole array is optically characterized using a home-built transmittance setup and an Ocean Optics visible spectrometer. The measured spectra (red solid lines) for x- and y-polarized incident light are displayed in Figs. 2(d) and 2(e), respectively. A plasmonic resonance can be observed for both polarizations around 600 nm wavelength. Importantly, this resonance overlaps with both transition lines of Eu^{3+} ($^5D_0 \rightarrow {}^7F_{1,2}$), as indicated by the green and red solid vertical lines in Figs. 2(d) and 2(e). Note that the subsequent deposition

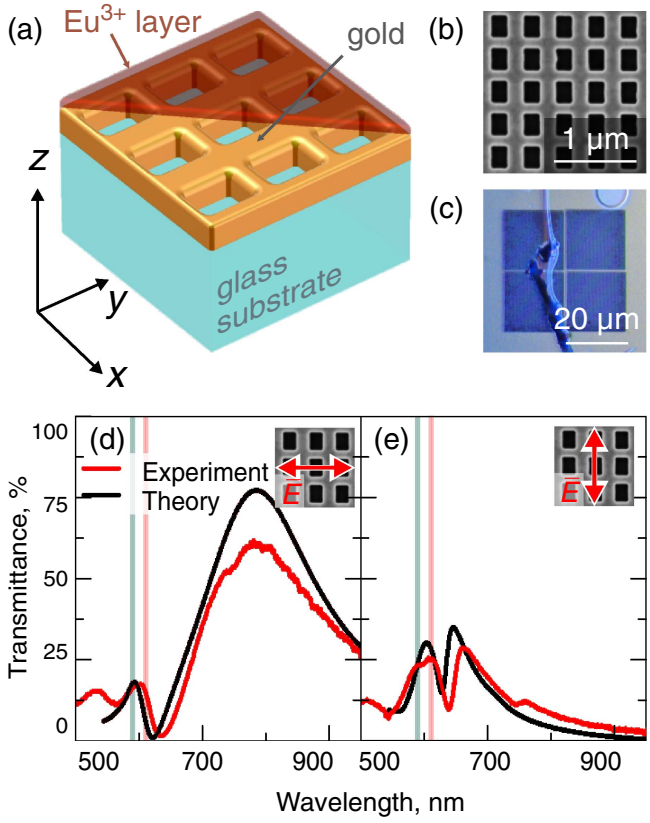

Fig. 2. (a) Sample geometry: a gold film with rectangular nanoholes supporting plasmonic resonances around 600 nm for both orthogonal polarizations is covered by a thin layer (red area) containing Eu^{3+} ions. (b) A SEM image of the nanohole array and (c) an optical microscope image of the sample with the deposited Eu^{3+} film. (d), (e) Experimentally measured (red solid line) and numerically calculated (black solid line) linear transmittance spectra of the sample for (d) x and (e) y polarizations.

of the Eu^{3+} thin film only negligibly red-shifts the spectral transmission spectrum of the nanohole array, as confirmed by numerical simulations using the commercial software package CST Microwave Studio. In the simulations, we use a semi-infinite glass substrate with a refractive index of $n = 1.5$ and for the permittivity of gold we use data from Ref. [27]. The calculated spectra [black solid lines in Figs. 2(d) and 2(e)] are in good agreement with the experimental results and well reproduce the resonances at 600 nm wavelength.

As the next step, we deposit a thin film of Eu(TTA)^3(L18) onto the sample using the Langmuir–Blodgett technique [5,28]. A light microscope image of the resulting sample is shown in Fig. 2(c). Chloroform solutions of Eu(TTA)^3(L18) and polystyrene were mixed in a proportion of 1:5. A 30 μl drop of the mixture solution was spread on water surface. After the evaporation of chloroform, a thin polymeric film was formed on the water surface. By immersing the sample from the top, a film with a uniform thickness of approximately 30–40 nm (measured by a profilometer) is transferred onto the sample surface with large area coverage of approximately 80 mm^2.

After the Eu(TTA)^3(L18) thin-film deposition, we analyzed the emission from Eu^{3+} electric and magnetic

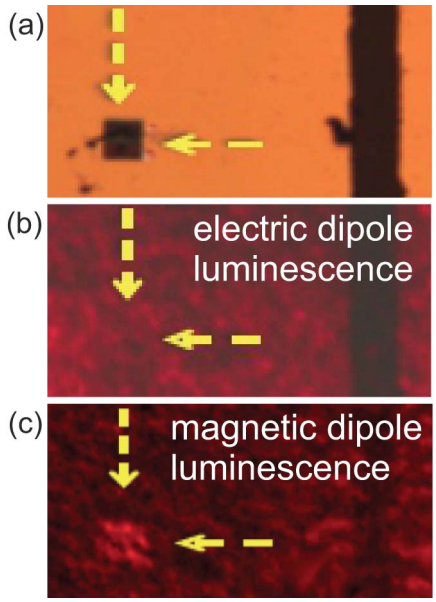

Fig. 3. (a) Image of the sample area of interest illuminated with white light. The dark square highlighted by the yellow dashed arrows is the nanohole array, while the dark stripe to the right is a region where the gold film has been removed by scratching. (b), (c) A photoluminescence microscope image [same area as in (a)] of Eu^{3+} at (b) $\lambda = 610$ nm (electric dipole transition) and (c) $\lambda = 590$ nm (magnetic dipole transition). The excitation wavelength is $\lambda = 325$ nm.

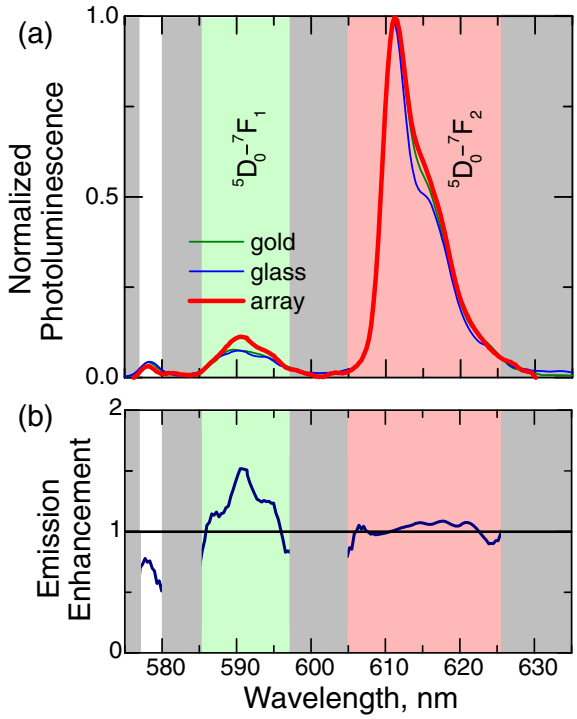

Fig. 4. (a) Emission spectra of the $Eu(TTA)^3(L18)$ film on top of the nanohole array (red solid line), the 150 nm thick gold film (green solid line), and the bare glass substrate (blue solid line). The spectra are normalized to the maximum of the electric dipole emission at 611 nm. (b) Emission enhancement, defined as the ratio of the normalized emission spectrum of Eu^{3+} over the nanohole array and the emission from Eu^{3+} over the plane gold surface, above the noise level.

dipole transitions in the presence of the plasmonic nanostructure. We first perform photoluminescence microscopy using a Zeiss Imager Z2 microscope equipped with an Axiocam camera, which allows simultaneous observation of the emission from Eu^{3+} deposited on different areas of the sample. Eu^{3+} is excited with a He–Cd laser at $\lambda = 325$ nm wavelength via a multimode step-index optical fiber (NA = 0.22, core diameter 200 μm). Interferometric narrow-band transmission filters (10 nm bandwidth) centered at 610 and 590 nm are inserted in the recording channel in order to separately collect the emission signals corresponding to the electric and magnetic dipole transitions.

A white-light microscope image of the area of interest is shown in Fig. 3(a). We chose the field of view such that it contains the nanohole array (marked by yellow dashed arrows) as well as two different reference areas: the gold film and a region of bare glass substrate obtained by scratching away the gold film in the vicinity of the array (dark stripe on the right). The distinct interactions of these reference areas with the electric and magnetic dipole emitters have been investigated in detail as a function of the gold film thickness [2–4,10–13]. It was concluded that for both electric and magnetic dipole transitions the emission from Eu^{3+} ions on top of a gold film with thickness exceeding 70 nm is brighter as compared with the emission on top of the bare glass substrate.

The recorded photoluminescence microscopy images for the 610 and 590 nm detection wavelengths for the same area as in Fig. 3(a) are displayed in Figs. 3(b) and 3(c). The image in Fig. 3(b) is recorded with the 610 nm filter and corresponds to the electric dipole transition. Here, a similar enhancement as for the metallic mirror is observed, such that the array cannot be distinguished from the surrounding gold film. In Fig. 3(c), which was recorded with the 590 nm filter at the wavelength of the magnetic dipole transition, in contrast, the array is seen as a bright square on the darker gold film background. We note that for emitters with high quantum yield, as in our case [5], the observed fluorescence enhancement can underestimate the actual radiative decay rate enhancement. In accordance with previous studies [12], we also find that the bare glass area looks darker than the gold film for both electric and magnetic dipole emission. This clearly indicates that the enhancement in magnetic transition observed in the vicinity of the nanohole array cannot merely be explained by the partial absence of gold and is a result of the resonant response of the nanoholes.

Next, we measure the emission spectra from the three different areas (nanohole array, gold film, and bare glass substrate). The emission spectra were recorded using an Ocean Optics PC2000 fiber optic spectrometer with a 400 μm diameter fiber optic probe. An objective lens (×10 magnification, 0.25 NA) was used to obtain a magnified image of the sample region of interest and project it onto the optical fiber probe. Figure 4(a) shows the three spectra, each normalized to the intensity of the dominant spectral line $^5D_0 \rightarrow {}^7F_2$ around 610 nm. The normalization allows assessing the changes in the relative emission intensities of the spectral lines. The

normalized spectra of Eu^{3+} emission on top of gold and on top of the glass look identical, whereas in the spectrum of Eu^{3+} on top of a nanohole array, the magnetic line $^5D_0 \rightarrow {}^7F_1$ becomes stronger. To emphasize the changes in the relative intensities of the Eu^{3+} lines, we plot in Fig. 4(b) the emission enhancement defined as the ratio of the spectra measured on top of the nanohole array and on top of gold. We observe over 50% enhancement of the magnetic line $^5D_0 \rightarrow {}^7F_1$ emission as compared with the dominant electric line $^5D_0 \rightarrow {}^7F_2$ emission.

In conclusion, an enhancement of magnetic dipole transition in the spontaneous emission spectrum of Eu^{3+} is observed in a system of a gold nanohole array featuring plasmonic resonances in the visible spectral range, designed to overlap with the magnetic and electric dipole transitions of Eu^{3+}. These findings present the first step toward using engineered plasmonic or dielectric nanostructures to obtain bright magnetic dipole emitters at optical frequencies.

We acknowledge the support by the National Science Foundation (NSF) PREM grant no. DMR 1205457, NSF IGERT grant no. DGE 0966188, the Army Research Office (ARO) grant W911NF-14-1-0639, the Australian National Fabrication Facility, and the Australian Research Council.

References

1. E. M. Purcell, Phys. Rev. **69**, 681 (1946).
2. N. Noginova, G. Zhu, M. Mayy, and M. A. Noginov, J. Appl. Phys. **103**, 07E901 (2008).
3. S. Karaveli and R. Zia, Phys. Rev. Lett. **106**, 193004 (2011).
4. X. Ni, G. V. Naik, A. V. Kildishev, Y. Barnakov, A. Boltasseva, and V. M. Shalaev, Appl. Phys. B **103**, 553 (2011).
5. R. Hussain, D. Keene, N. Noginova, and M. Durach, Opt. Express **22**, 7744 (2014).
6. L. Aigouy, A. Cazé, P. Gredin, M. Mortier, and R. Carminati, Phys. Rev. Lett. **113**, 076101 (2014).
7. B. Rolly, B. Bebey, S. Bidault, B. Stout, and N. Bonod, Phys. Rev. B **85**, 245432 (2012).
8. S. M. Hein and H. Giessen, Phys. Rev. Lett. **111**, 026803 (2013).
9. K. H. Drexhage, J. Lumin. **1–2**, 693 (1970).
10. W. Lukosz and R. E. Kunz, J. Opt. Soc. Am. **67**, 1607 (1977).
11. W. Lukosz, J. Opt. Soc. Am. **69**, 1495 (1979).
12. N. Noginova, Y. Barnakov, H. Li, and M. A. Noginov, Opt. Express **17**, 10767 (2009).
13. S. Karaveli and R. Zia, Opt. Lett. **35**, 3318 (2010).
14. T. H. Taminiau, S. Karaveli, N. F. Hulst van, and R. Zia, Nat. Commun. **3**, 979 (2012).
15. S. Karaveli, A. J. Weinstein, and R. Zia, Nano Lett. **13**, 2264 (2013).
16. N. Noginova, R. Hussain, M. A. Noginov, J. Vella, and A. Urbas, Opt. Express **21**, 23087 (2013).
17. K. H. Drexhage, "Interaction of light with monomolecular dye layers," in *Progress in Optics*, E. Wolf, ed. (Elsevier, 1974), Vol. **12**, pp. 163–232.
18. M. A. Noginov and V. A. Podolskiy, eds., *Tutorials in Metamaterials* (CRC Press, Taylor & Francis Group, 2011).
19. S. Linden, C. Enkrich, M. Wegener, J. Zhou, T. Koschny, and C. M. Soukoulis, Science **306**, 1351 (2004).
20. I. Staude, A. E. Miroshnichenko, M. Decker, N. T. Fofang, S. Liu, E. Gonzales, J. Dominguez, T. S. Luk, D. N. Neshev, I. Brener, and Y. Kivshar, ACS Nano **7**, 7824 (2013).
21. H. W. Kihm, S. M. Koo, Q. H. Kim, K. Bao, J. E. Kihm, W. S. Bak, S. H. Eah, C. Lienau, H. Kim, P. Nordlander, N. J. Halas, N. K. Park, and D. S. Kim, Nat. Commun. **2**, 451 (2011).
22. E. Devaux, A. Dereux, E. Bourillot, J. C. Weeber, Y. Lacroute, J. P. Goudonnet, and C. Girard, Phys. Rev. B **62**, 10504 (2000).
23. D. Denkova, N. Verellen, A. V. Silhanek, V. K. Valev, P. V. Dorpe, and V. V. Moshchalkov, ACS Nano **7**, 3168 (2013).
24. H. W. Kihm, J. Kim, S. Koo, J. Ahn, K. Ahn, K. Lee, N. Park, and D. S. Kim, Opt. Express **21**, 5625 (2013).
25. B. le Feber, N. Rotenberg, D. M. Beggs, and L. Kuipers, Nat. Photonics **8**, 43 (2014).
26. V. I. Tsaryuk, K. P. Zhuravlev, V. F. Zolin, V. A. Kudryashova, J. Legendziewicz, and R. Szostak, J. Appl. Spectrosc. **74**, 51 (2007).
27. P. B. Johnson and R. W. Christy, Phys. Rev. B **6**, 4370 (1972).
28. K. Wang, L. Gao, and C. Huang, J. Photochem. Photobiol. A **156**, 39 (2003).